

Chromosome Segregation Impacts on Cell Growth and Division Site Selection in *Corynebacterium glutamicum*

Catriona Donovan^{1,2}, Astrid Schauss³, Reinhard Krämer², Marc Bramkamp^{1,2*}

1 Department of Biology I, Ludwig-Maximilians-University Munich, Planegg-Martinsried, Germany, **2** Institute for Biochemistry, University of Cologne, Cologne, Germany, **3** Cologne Excellence Cluster on Cellular Stress Response in Aging-Associated Diseases (CECAD), Cologne, Germany

Abstract

Spatial and temporal regulation of bacterial cell division is imperative for the production of viable offspring. In many rod-shaped bacteria, regulatory systems such as the Min system and nucleoid occlusion ensure the high fidelity of midcell divisome positioning. However, regulation of division site selection in bacteria lacking recognizable Min and nucleoid occlusion remains less well understood. Here, we describe one such rod-shaped organism, *Corynebacterium glutamicum*, which does not always place the division septum precisely at midcell. Here we now show at single cell level that cell growth and division site selection are spatially and temporally regulated by chromosome segregation. Mutants defective in chromosome segregation have more variable cell growth and aberrant placement of the division site. In these mutants, division septa constrict over and often guillotine the nucleoid, leading to nonviable, DNA-free cells. Our results suggest that chromosome segregation or some nucleoid associated factor influences growth and division site selection in *C. glutamicum*. Understanding growth and regulation of *C. glutamicum* cells will also be of importance to develop strains for industrial production of biomolecules, such as amino acids.

Citation: Donovan C, Schauss A, Krämer R, Bramkamp M (2013) Chromosome Segregation Impacts on Cell Growth and Division Site Selection in *Corynebacterium glutamicum*. PLoS ONE 8(2): e55078. doi:10.1371/journal.pone.0055078

Editor: Dirk-Jan Scheffers, University of Groningen, Groningen Institute for Biomolecular Sciences and Biotechnology, The Netherlands

Received: October 5, 2012; **Accepted:** December 18, 2012; **Published:** February 6, 2013

Copyright: © 2013 Donovan et al. This is an open-access article distributed under the terms of the Creative Commons Attribution License, which permits unrestricted use, distribution, and reproduction in any medium, provided the original author and source are credited.

Funding: These authors have no support or funding to report.

Competing Interests: The authors have declared that no competing interests exist.

* E-mail: marc.bramkamp@lmu.de

Introduction

Many rod-shaped bacteria divide precisely at midcell, generating two equally sized and genetically identical daughter cells. Division site selection is controlled by regulating the positioning of the primary bacterial cell division protein, FtsZ. This tubulin homologue polymerizes at midcell forming a ring-like structure known as the Z-ring, which subsequently primes the midcell for assembly of the division machinery complex [1,2]. Spatial regulators, such as the Min system and nucleoid occlusion, facilitate midcell localization of the Z-ring and, subsequently, the divisome [3]. The effector proteins of nucleoid occlusion, Noc in *B. subtilis* and SlmA in *E. coli*, are DNA-binding proteins that prevent Z-ring formation over the nucleoid [4,5,6]. The Min system prevents aberrant divisions close to the cell poles [7,8]. In *E. coli*, the Min system oscillates pole to pole, thereby setting up a gradient of the FtsZ inhibitor, MinC, which is lowest at midcell [3,9,10,11,12]. The *B. subtilis* Min system does not oscillate and has been recently shown to be important for disassembly of the divisome machinery and prevents new rounds of cytokinesis occurring close to the original cell division site [13,14].

Assembly of the divisome must be temporally coordinated with chromosome replication and segregation to ensure maintenance of genomic integrity. Bacterial DNA segregation is often mediated by the tripartite partitioning system encoded by the *par* locus. Two *trans*-acting proteins, encoded in an operon (*parA* and *parB*, respectively), and *cis*-acting “centromere-like” elements, found scattered around the origin of replication (*oriC*), constitute the Par segregation machinery [15,16,17]. The centromere-binding pro-

tein (ParB) binds the centromere-like element (*parS*) forming a nucleoprotein complex [18]. Dynamic localization of the Walker type P-loop ATPase (ParA), has been suggested to mediate segregation of the ParB-*parS* nucleoprotein complexes [19].

In the absence of recognizable homologues of the Min system and nucleoid occlusion (Noc or SlmA), bacteria have developed alternative strategies to spatially and temporally regulate cell division. A well-studied example is *Caulobacter crescentus*, which strictly synchronises chromosome segregation with cell division [20,21]. In the predivision cell, the negative regulator of Z-ring polymerization, MipZ, forms a gradient extending from the origin tethered pole towards the midcell region [22]. ParB is imperative in maintenance of MipZ gradients [22,23]. After replication onset and as the chromosome segregates, MipZ travels with the segregating ParB bound origin. At the opposite cell pole, MipZ displaces FtsZ, restricting Z-ring polymerization to the midcell region. Thus, in *C. crescentus* null deletion mutants of the Par system are lethal [24].

Members of the Actinobacteria phylum, such as *Corynebacterium glutamicum*, not only lack homologues of Min and nucleoid occlusion, but also other positive and negative regulators of FtsZ, such as ErzA, FtsA, ZapA or ZipA [25]. Interestingly, the placement of the division septum in this rod-shaped organism is relatively flexible and is not necessarily always positioned precisely at midcell. Previously, we found that the ParAB system works as chromosome partitioning system [26]. Here, cell growth and division site selection in *C. glutamicum* was analyzed at the single cell level. By contrast to wild type cells, in the absence of an active

chromosome segregation machinery, disorganised chromosomes additionally impacts on division site selection and growth.

Results

Growth of *C. glutamicum* is Regulated by a Size-based Mechanism

Conventionally, growth characterisation of microbial cells involved analysis of cell populations as a whole, which, although overall informative, neglect potential single cell variability. In recent years, live cell imaging has been employed to address heterogeneity at the single cell level [27,28,29]. We assessed the growth characteristics of *C. glutamicum* at the single cell level by means of live cell imaging. For this purpose microfluidic chambers were employed. These chambers are designed to hold cells at a single focal plane while supplying cells with a continuous flow of nutrients permitting monitoring of cell cycle events over multiple generations. To allow for accurate measurements and subsequently unambiguously define the cell poles and division septa, we made use of a DivIVA-mCherry expressing strain, where expression is under the control of the native promoter (Movie S1) [30]. In *C. glutamicum*, DivIVA localises at the cell poles and is recruited at a late stage to the mature division septum, which after completion of division forms the new cell pole [31].

Growth of the DivIVA-mCherry expressing strain was assessed by measuring the increase in cell length per unit time directly after one division event (cell birth) until directly before the next division event. The elongation rate is in the range of 1 to 3.25 $\mu\text{m}/\text{h}$, averaging at 1.9 $\mu\text{m}/\text{h}$ and follows a Gaussian distribution (Fig. 1A). Although cell division in *C. glutamicum* does not necessarily give rise to two equally sized daughter cells, the Gaussian distribution of elongation rates would suggest that the birth length, determined by the placement of the division septum, and the elongation rate are correlated. Indeed, plotting the birth length (size of cell directly after division) against the elongation length (the increase in cell length between two related division events) demonstrated that these two parameters are associated. The birth length of *C. glutamicum* cells ranges between 1.5 and 2.5 μm and these cells subsequently double in size (ranging from 1 to 2.5 μm) before the next division event takes place (Fig. 1A). Taken together, these data show that wild type *C. glutamicum* cells retain a relatively homogenous size both at birth and prior to division.

To assess the functionality of the DivIVA-mCherry fusion, the growth characteristics of wild type *C. glutamicum* was measured (Fig. S1 and Movie S2). Similar to the DivIVA-mCherry strain, the elongation rate of wild type cells follows a Gaussian distribution (Fig. 1A). The elongation rate ranges from 1 to 3.25 $\mu\text{m}/\text{h}$, however the average elongation rate of the wild type strain is increased compared to the DivIVA-mCherry strain (2.4 $\mu\text{m}/\text{h}$ and 1.9 $\mu\text{m}/\text{h}$, respectively). The association of the birth length and the elongation length revealed a comparable association when compared to the DivIVA-mCherry strain (Fig. 1B). Considering that DivIVA is involved in a number of cellular processes in *C. glutamicum*, the results presented above show that the DivIVA-mCherry fusion is largely functional.

The relationship between birth length and elongation length has been used to broadly define the mechanism that regulates the timing of division events [28,32]. If birth lengths negatively correlate with elongation length, a size-based regulatory mechanism is responsible. On the other hand, a time-based mechanism shows no correlation between birth length and elongation length. Using this approach it was recently demonstrated that *Mycobacterium* cells employ a time-based mechanism, while *E. coli* cells

employ a size-based mechanism [28]. When assessed for wild type *C. glutamicum* or the DivIVA-mCherry strain, we found that birth lengths negatively correlate with elongation lengths, suggesting that a size-based or a mixed regulatory mechanism is employed (Fig. 1B).

Chromosome Segregation Impacts on Cell Growth in *C. glutamicum*

Mutation of the *C. glutamicum* chromosome segregation machinery (*parA* or *parB*) induce a plethora of phenotypes, including altered growth rates and cell lengths, anucleate cells, guillotined chromosomes and perturbed chromosome organization [26]. These phenotypic consequences led us to speculate that chromosome segregation and/or organization might be coupled to division site selection and cell growth. With this in mind, the growth characteristics of *parA* and *parB* mutants were analyzed using live cell imaging (Fig. S1, Movies S3 and S4). Therefore, a divIVA-mCherry fusion was introduced into markerless *parA* or *parB* deletion background strains.

In cells lacking *parA* or *parB*, elongation rates varied from the DivIVA-mCherry strain (Fig. 1A, $F < 0.05$). In the absence of *parA*, the elongation rate is reduced, while more variability is observed for the *parB* mutant, ranging from 0.25 $\mu\text{m}/\text{h}$ to greater than 5 $\mu\text{m}/\text{h}$. Variation in the elongation rate might be due to deviating cell lengths at birth. Shorter cells at birth would require more time to reach a threshold size, while longer cells would require less time. Therefore, the association between birth length and elongation length was measured. In the absence of *parA* or *parB*, both birth lengths and elongation lengths are more variable (Fig. 1B). However, birth and elongation lengths remain negatively correlated. Taken together, mutation of *parA* or *parB* not only alters chromosome organization, but also gives rise to a population of cells that is extremely heterogeneous both in birth size and elongation rate.

Chromosome Segregation Influences Division Site Selection in *C. glutamicum*

The inconsistency of cell lengths at birth between wild type or DivIVA-mCherry and *par* mutant cells would suggest that the placement of the division septum is more variable in the absence of functional chromosome segregation machinery. As *C. glutamicum* lacks recognisable homologues of the conventional division site regulatory systems and no other positive or negative regulation of cell division are presently known, we speculated that chromosome segregation or the subcellular organization of the nucleoid might influence division site selection.

On a single cell level, the placement of the division site in *C. glutamicum* cells was spatially (division symmetry) and temporally (timing of division events) assessed. Division symmetry was assessed by measuring the distance between the division septum and the nearest cell pole divided by the length of the cell, with 0.5 corresponding to the exact midcell. We found that the placement of the division site is not always precisely at midcell in wild type or DivIVA-mCherry cells; but some regulatory mechanism must exist because the division septum is sited in the region between the 1/3 and 2/3 positions of the cell (Fig. 2A). In the DivIVA-mCherry strain, we observed polar divisions occurring in a low percentage of the cells (0.3%) (Table 1). As DivIVA has been proposed to anchor the *oriC* at the cell poles through interaction with ParB, the low frequency of polar divisions is likely a consequence of the mCherry fusion which results in a mild chromosome segregation (anchoring) defect. However, in the absence of *parA* or *parB*, the placement of the division site is significantly more variable (Fig. 2A;

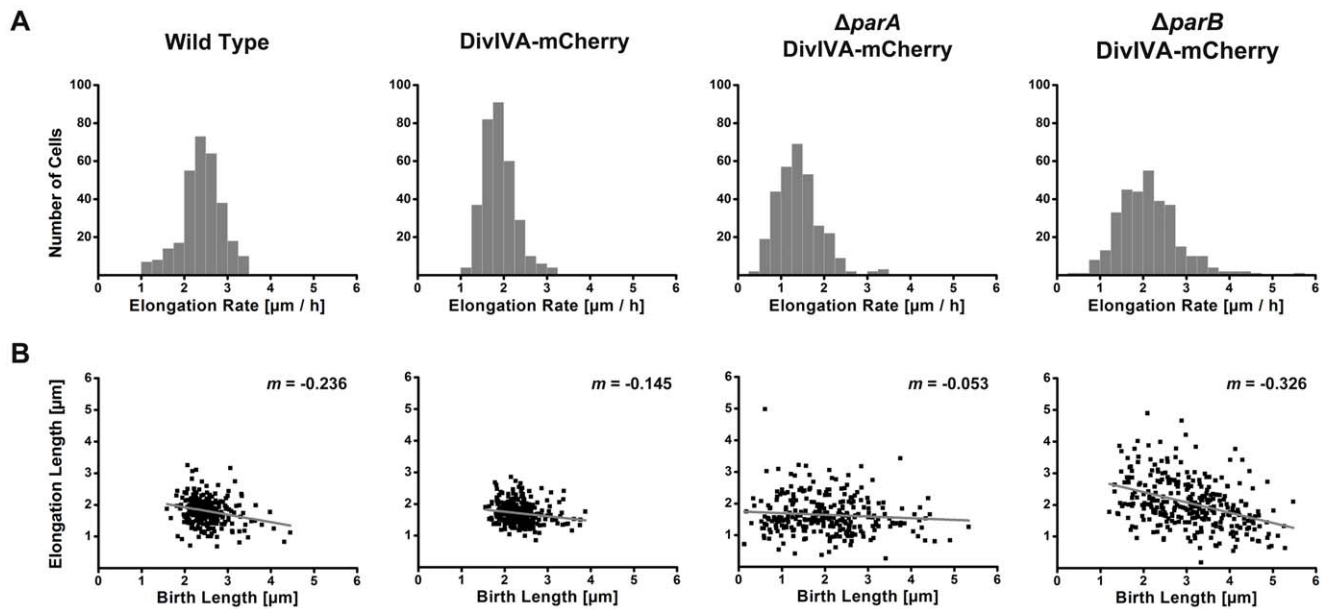


Figure 1. Chromosome segregation defects lead to altered growth in *C. glutamicum*. (A) Distribution of elongation rates of wild type, DivIVA-mCherry, $\Delta parA$ DivIVA-mCherry and $\Delta parB$ DivIVA-mCherry mutant cells. ($n \geq 300$). (B) Association of birth lengths and elongation lengths in DivIVA-mCherry, $\Delta parA$ DivIVA-mCherry and $\Delta parB$ DivIVA-mCherry. In wild type and DivIVA-mCherry cells the birth length and elongation length are associated. In the absence of *parA* or *parB*, more variation in the length of the cell at birth and the cell length before division is observed. Negative correlation between birth and elongation lengths indicates a size-based cell cycle regulatory mechanism (grey line). Regression line slope is shown on top right. ($n \geq 300$).

doi:10.1371/journal.pone.0055078.g001

$F < 0.05$). The frequency of polar cell division is drastically increased, often giving rise to nonviable, DNA-free cells (Table 1). Tracking division events over a number of generations revealed that divisions close to one cell pole often occurred repeatedly at the same pole. In almost every cell lineage analysed, in particular in the case of the *parA* mutant, asymmetric polar division was observed.

In wild type and DivIVA-mCherry cells, the birth length and elongation length are correlated (Fig. 1B). Thus, starting from a single cell this would suggest that the timing of birth events would also be relatively synchronous. Indeed, at least for a number of generations, division events occur at regular intervals (Fig 2B). As outlined above, growth of the DivIVA-mCherry strain is reduced compared to the wild type (Fig. 1A). As a consequence, the timing of division events is delayed in the DivIVA-mCherry strain. Note that after 3 hours four division events take place in the wild type cells, while in the DivIVA-mCherry strain three division events are observed (Fig 2B). Nevertheless, in both strains division occurs at regular intervals. It should be pointed out that after some time a microcolony is formed, and in these microcolonies nutrient availability and growth are altered compared to single cells. In contrast, cells lacking *parA* or *parB* have more variable birth lengths and elongation lengths, and subsequently the timing of division events is random (Fig 2B). This result strongly indicates that alterations in chromosome localization, as a consequence of *parA* or *parB* mutation, directly influence cell growth and division site placement in *C. glutamicum*.

Defects in Chromosome Segregation Lead to Chromosome Fragmentation

Next, we wanted to visualize the nucleoid localization and dynamics during live cell imaging, in particular in the absence of *parA* or *parB*. Cells were grown in the microfluidic chamber for a number of generations prior to staining cells with Hoechst DNA

stain. As the DNA stain is somewhat toxic, growth of the cells is impaired. However, division events that have been initiated prior to addition of Hoechst stain are completed and hence, allow visualization of septum constriction over the chromosome.

In wild type and DivIVA-mCherry cells, each daughter cell always contained a nucleoid. However, in the *parA* or *parB* mutant strains, a high frequency of anucleate cells were observed (Table 1). Additionally, constriction of the division septum over the nucleoid was observed. In the case of $\Delta parA$ 9% of the division septa constricted over the chromosome, while in the case of $\Delta parB$ 10.5% was observed ($n \geq 650$). In the example shown (Fig. 3 and Movie S5), the division septum is positioned over the nucleoid and as the septum begins constricting the DNA is pumped into the cell half containing the bulk of the chromosome. DNA translocases, such as FtsK in *E. coli*, coordinate the late stages of cytokinesis and chromosome segregation ensuring that DNA does not get trapped in the inward growing septum [33,34]. *C. glutamicum* contains a homolog of FtsK, however it has not been studied in detail, to date. Nevertheless, in the example shown DNA translocase did not succeed in clearing the DNA from the invaginating septum. Subsequently, part of the chromosome was fragmented and then degraded. Our results confirm earlier postulations [35] that *C. glutamicum* likely lacks a nucleoid occlusion protein, such as SlmA or Noc.

Discussion

Most of our knowledge on bacterial growth and cell division has been derived from the rod-shaped model organisms such as *B. subtilis* and *E. coli*. However, many of the symmetry generating molecular rulers are lacking in other rod-shaped bacteria, for example the rod-shaped actinomycete *C. glutamicum*. Here, growth and division site selection in *C. glutamicum* was analyzed at the single cell level.

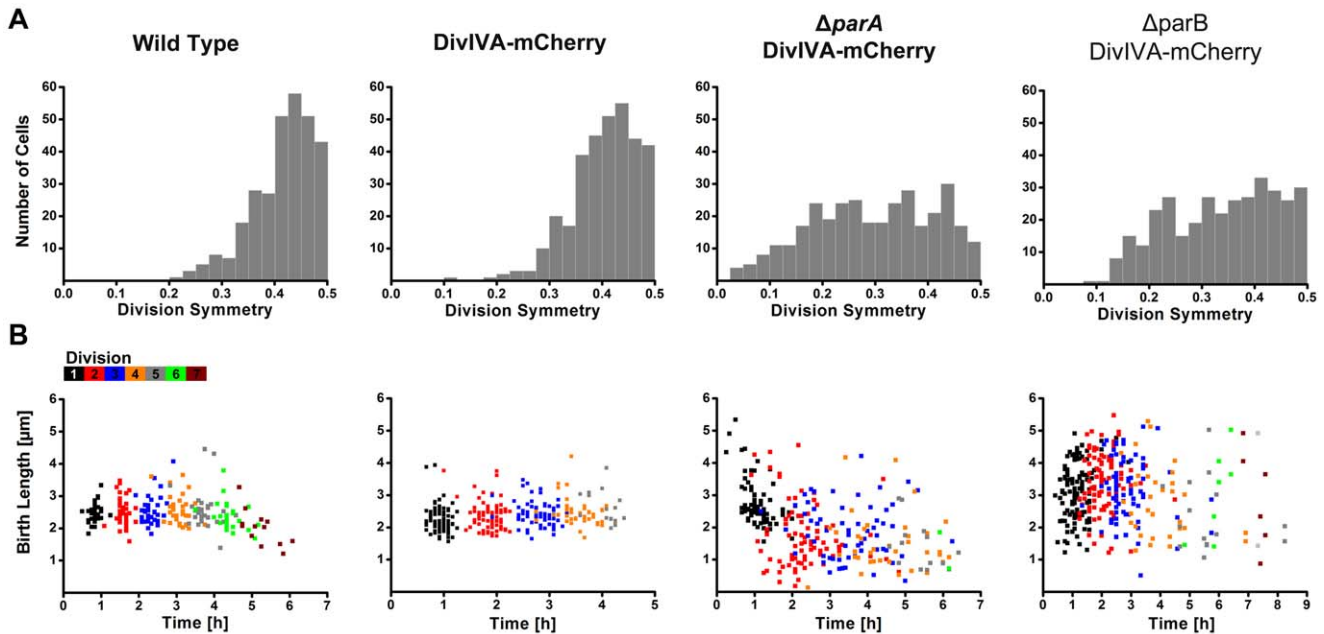


Figure 2. Chromosome segregation influences spatial and temporal control of cell division. (A) Distribution of division site placement in wild type, DivIVA-mCherry, $\Delta parA$ DivIVA-mCherry and $\Delta parB$ DivIVA-mCherry cells. In wild type and DivIVA-mCherry cells, division septa are placed near the midcell. In the absence of *parA* or *parB*, the positioning of division septa is more variable ($F > 0.05$). ($n \geq 300$). (B) Timing of birth events in wild type, $\Delta parA$ and $\Delta parB$ cells. In wild type and DivIVA-mCherry cells, division occurs at regular time intervals. Note that after 3–4 generations a microcolony is formed. In the absence of *parA* or *parB*, the time at which division occurs is random. In addition, the length of cells at birth is much more variable compared to wild type cells. ($n \geq 250$).
doi:10.1371/journal.pone.0055078.g002

Cell elongation in many rod-shaped bacteria involves intercalation of new peptidoglycan into the lateral cell wall [36,37,38]. The actin cytoskeleton is not only imperative to this mode of growth but also to the maintenance of rod-shape [39,40,41,42]. By contrast, Actinobacteria, which lack an MreB-based cell elongation machinery, insert new cell wall material at the cell poles, giving rise to an apical mode of cell elongation [25,31,43]. Apical growth in Actinomycetes has been reported to be organized by DivIVA [31,43,44]. In this study, the localization pattern of DivIVA was exploited to mark the cell poles and constricting division septa in growing *C. glutamicum* cells.

E. coli and *B. subtilis* cells normally exhibit little size variation under steady state conditions [45,46]. Heterogeneity in cell size could arise from alterations in the placement of the division septum. Thus, regulating the placement of the division site additionally helps maintain a homogenous cell size. By contrast, asymmetry in division site selection as well as polar cell growth was shown for mycobacterial cells [28]. Such asymmetry results

in an extremely heterogeneous population of cells with diverse susceptibility to antibiotics. In *C. glutamicum*, cell division does not always give rise to equally sized daughter cells (Fig. 2A). Although the majority of cells divide close to the midcell region, the fraction of cell dividing off-centre could lead to cell size heterogeneity. Interestingly, we find that the growth rate of *C. glutamicum* cells follows a Gaussian distribution, ranging between 1–3.5 $\mu\text{m}/\text{h}$ (Fig. 2A). To gain additional information on the homo- or heterogeneity of the population, the association of birth lengths and elongation lengths was assessed. Good correlation between birth and elongation lengths was observed, suggesting that *C. glutamicum* maintains a relatively homogenous cell size both prior to and after division (Fig. 1B). Variability in division site placement must be compensated for by increased or decreased growth rate, maintaining a threshold cell size before the next division event occurs. This finding is in line with the observation that birth lengths negatively correlate with elongation length, suggesting that *C. glutamicum* employs a size-based regulatory mechanism. However, we also observe that division events occur with relative precise timing in wild type *C. glutamicum* cells. This would suggest that *C. glutamicum* employs a mixture of time- and size-based regulatory mechanisms. This is an interesting difference to growth control to the closely related *Mycobacteria*. For *M. smegmatis* and *M. tuberculosis* only a time-based mechanism was proposed [28]. A major difference in the lifestyle between *Corynebacteria* and *Mycobacteria* is that *Corynebacteria* grow with much higher growth rates. Thus, it seems plausible that these cells not only rely on one control mechanism, but rather follow a mixed strategy to avoid that cells where division failed will grow out to large filaments.

In the absence of an apparent Min system and a clear Noc/SlmA homologue, how is division site regulated in *C. glutamicum*? We previously reported that mutation of the *parAB* partition

Table 1. Anucleate cells and polar divisions in wild type *C. glutamicum* and *par* mutants.

	Anucleate cells ($n \geq 650$)	Polar divisions ($n \geq 300$)
Wild Type	0%	0%
DivIVA-mCherry	0%	0.3%
$\Delta parA$ DivIVA-mCherry	18%	12%
$\Delta parB$ DivIVA-mCherry	28%	3.5%

doi:10.1371/journal.pone.0055078.t001

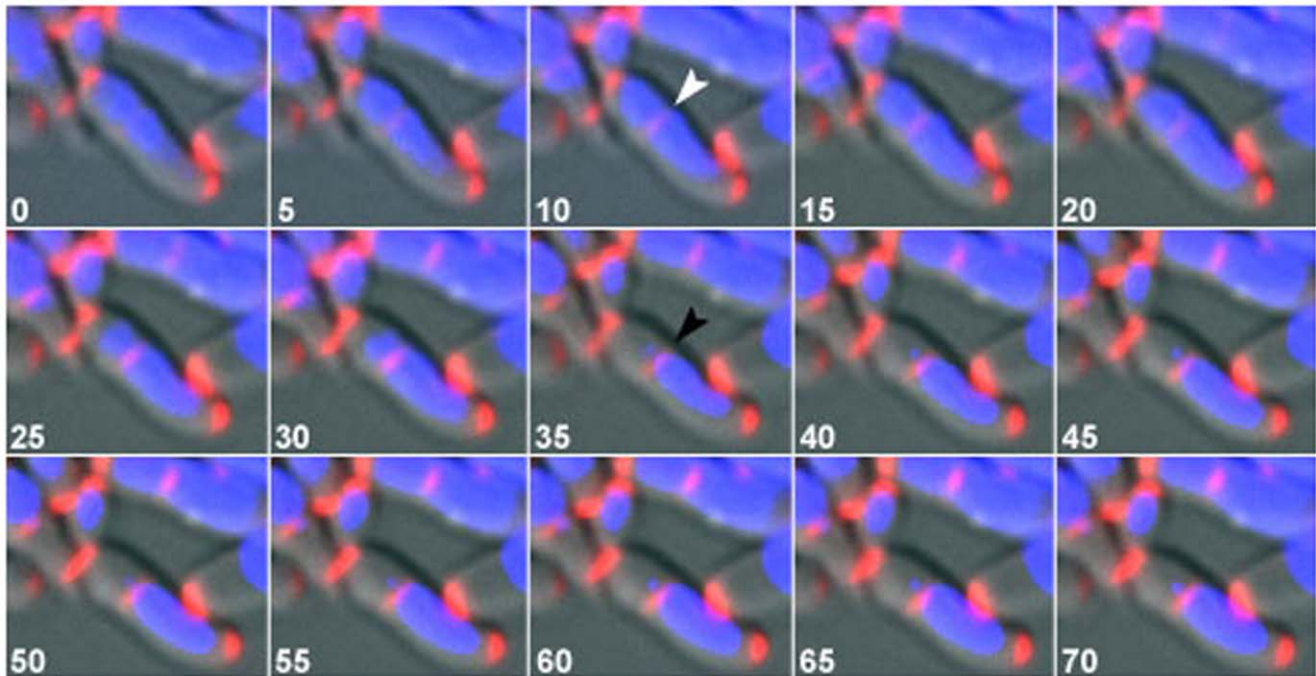


Figure 3. In the absence of *parB*, division septa constrict over the nucleoid, guillotining part of the chromosome. Shown is a time lapse series of DivIVA-mCherry expressing cell in the absence of *parB*. Images were acquired every 5 minutes and time points are indicated for each time frame. DNA is stained with Hoechst (blue) and DivIVA-mCherry is shown in red. DivIVA-mCherry is recruited to the division septum, which has assembled over the chromosome (white arrowhead). The chromosome is pumped in one direction, into the cell half containing the bulk of the chromosome. The division septum constricts directly over part of the chromosome, leading to guillotining part of the chromosome (black arrowhead). See also Movie S5.

doi:10.1371/journal.pone.0055078.g003

system resulted in altered cell length distributions, aberrant placement of the division septa and a high frequency of anucleate cells [26]. When analyzed at the single cell level, we observed much more variability in division site selection, high frequency of polar divisions, along with significantly more variable birth lengths that do not correlate with elongation length. Although we do not know the molecular mechanism(s) that regulate growth and division site selection in *C. glutamicum*, we speculate that the nucleoid itself or some aspect associated with the nucleoid influences these parameters.

From the data presented here it appears that cell division and chromosome segregation are coupled in *C. glutamicum*. In *B. subtilis*, blocking cell division by overexpression of the Min system results in long filamentous cells with regularly spaced and segregated chromosomes. Conversely, mutation of *spo0J* (*parB*) or *soj* (*parA*) do not lead to severe cell division defects, approximately 2% anucleate cells result from mutation of *spo0J* [47]. Thus, cell division and chromosome segregation can be uncoupled in *B. subtilis*, probably as a consequence of partially overlapping cell cycle regulatory mechanisms.

A growing body of evidence suggests that the nucleoid morphology directly influences Z-ring positioning [22,24,48,49,50,51,52]. Blocking DNA replication at different stages induces different nucleoid morphologies which influence Z-ring positioning [49]. Thus, even in *B. subtilis*, *E. coli* and *C. crescentus* additional factors, potentially related to chromosome replication or the nucleoid structure, prime the midcell for Z-ring polymerization [48]. In line with these observations, alterations in the nucleoid structure lead to aberrant placement of the division site, in *C. glutamicum*.

Materials and Methods

Bacterial Strains

Bacterial strains and plasmids used in this study are listed in table 2.

Strain CDC025 was generated by transforming strain CDC001 ($\Delta parA$) with the plasmid pCD191 (DivIVA-mCherry) via electroporation. This strain contains an in-frame deletion of *parA* and expression of a DivIVA-mCherry fusion from the native promoter. Plasmid pCD191 is a pK19mobsacB derivative, which is non-replicative in *C. glutamicum* [26,54]. Chromosomal integration of the *mCherry* gene at the 3' end of the *divIVA* locus occurs via a two-step homologous recombination. The initial chromosome integration step was selected for on kanamycin plates. The second round of recombination was selected for by growth on 10% sucrose. Single colonies were isolated and tested for kanamycin sensitivity. Chromosomal integration of *mCherry* was confirmed by PCR.

Time-lapse Microscopy with Microfluidic Chambers

Live cell imaging was carried out in B04A microfluidic chamber (Onix, CellASIC). *C. glutamicum* cells were grown in BHI medium overnight. The next morning, cultures were diluted to OD₆₀₀ 1.0 and grown further in shaking flasks to approximately OD₆₀₀ 5.0. Cultures were diluted to OD₆₀₀ 0.005–0.01 prior to loading microfluidic chamber. Cells were loaded to wells with 5 psi for 10 seconds. Nutrient supply was maintained at 3 psi. The temperature was maintained at 30°C. Cells were grown in BHI during time lapse analysis and images were acquired at five minute intervals. For anucleate cell measurements and analysis of constricting division septa over the chromosome, cells were stained with Hoechst DNA stain (1 $\mu\text{g}/\text{ml}^{-1}$). Images were taken on a Delta Vision RT microscope (Applied Precision), using the softworX

Table 2. Bacterial strains and plasmids.

Strains	Relevant characteristics	Reference/source
<i>C. glutamicum</i> RES 167	Restriction deficient <i>C. glutamicum</i> mutant, otherwise considered wild type	[53]
CDC010	RES 167 derivative with <i>divIVA</i> -mCherry	[30]
CDC025	RES 167 Δ <i>parA</i> , <i>divIVA</i> -mCherry	This study
CDC012	RES 167 Δ <i>parB</i> , <i>divIVA</i> -mCherry	[30]
Plasmids	Relevant characteristics	Reference/source
pK19mobsacB	Integration vector, <i>ori</i> pUC, Km ^r , <i>mob sacB</i>	[54]
pK19mobsacB- Δ <i>parA</i>	Integration vector, <i>ori</i> pUC, Km ^r , <i>mob sacB</i> , Δ <i>parA</i>	[26]
pK19mobsacB- Δ <i>parB</i>	Integration vector, <i>ori</i> pUC, Km ^r , <i>mob sacB</i> , Δ <i>parB</i>	[26]
pCD191	Integration vector, <i>ori</i> pUC, Km ^r , <i>mob sacB</i> <i>divIVA</i> -mCherry	[26]

doi:10.1371/journal.pone.0055078.t002

software. Final image preparation was done using Volocity, Adobe Photoshop 6.0 (Adobe Systems Incorporated) or FIJI.

Statistical Analysis

All cell length measurements were acquired manually. Two-sample for variances F-test were calculated using Excel to determine the variability in distribution between wild type/*DivIVA*-mCherry and Δ *parA* or Δ *parB*.

Supporting Information

Figure S1 Still images of *DivIVA*-mCherry and *par* mutants grown in microfluidic chambers. Shown are still images of (A) *DivIVA*-mCherry, (B) Δ *parB* *DivIVA*-mCherry and (C) Δ *parA* *DivIVA*-mCherry. The arrows in (C) show a cell where the division septum is positioned close to the cell pole. In the same cell, the division septum in the following division event is also positioned close to the same cell pole. Time points are indicated in minutes on the top left corner. (TIF)

Movie S1 Growth of *C. glutamicum DivIVA*-mCherry cells. Images were acquired every five minutes for the total of 5 hours. (AVI)

References

- Bi EF, Lutkenhaus J (1991) FtsZ ring structure associated with division in *Escherichia coli*. *Nature* 354: 161–164.
- Wang X, Lutkenhaus J (1993) The FtsZ protein of *Bacillus subtilis* is localized at the division site and has GTPase activity that is dependent upon FtsZ concentration. *Mol Microbiol* 9: 435–442.
- Bramkamp M, van Baarle S (2009) Division site selection in rod-shaped bacteria. *Curr Opin Microbiol* 12: 683–688.
- Bernhardt TG, de Boer PA (2005) SlmA, a nucleoid-associated, FtsZ binding protein required for blocking septal ring assembly over Chromosomes in *E. coli*. *Mol Cell* 18: 555–564.
- Wu IJ, Ishikawa S, Kawai Y, Oshima T, Ogasawara N, et al. (2009) Noc protein binds to specific DNA sequences to coordinate cell division with chromosome segregation. *Embo J* 28: 1940–1952.
- Wu IJ, Errington J (2004) Coordination of cell division and chromosome segregation by a nucleoid occlusion protein in *Bacillus subtilis*. *Cell* 117: 915–925.
- de Boer PA, Crossley RE, Rothfield LI (1988) Isolation and properties of *minB*, a complex genetic locus involved in correct placement of the division site in *Escherichia coli*. *J Bacteriol* 170: 2106–2112.
- de Boer PA, Crossley RE, Rothfield LI (1989) A division inhibitor and a topological specificity factor coded for by the minicell locus determine proper placement of the division septum in *E. coli*. *Cell* 56: 641–649.
- Hu Z, Lutkenhaus J (1999) Topological regulation of cell division in *Escherichia coli* involves rapid pole to pole oscillation of the division inhibitor MinC under the control of MinD and MinE. *Mol Microbiol* 34: 82–90.
- Raskin DM, de Boer PA (1999) MinDE-dependent pole-to-pole oscillation of division inhibitor MinC in *Escherichia coli*. *J Bacteriol* 181: 6419–6424.

Movie S2 Growth of wild type *C. glutamicum* cells. Images were acquired every five minutes for the total of 5 hours. (M4V)

Movie S3 Growth of *C. glutamicum* Δ *parA* *DivIVA*-mCherry cells. Images were acquired every 5 minutes for a total of 7 hours. (AVI)

Movie S4 Growth of *C. glutamicum* Δ *parB* *DivIVA*-mCherry cells. Images were acquired every 5 minutes for a total of 3 hours 40 minutes. (AVI)

Movie S5 In cells lacking *parB*, the division septum guillotines part of the chromosome. (AVI)

Author Contributions

Conceived and designed the experiments: CD AS RK MB. Performed the experiments: CD AS RK MB. Analyzed the data: CD AS RK MB. Contributed reagents/materials/analysis tools: CD AS RK MB. Wrote the paper: CD AS RK MB.

- Hale CA, Meinhardt H, de Boer PA (2001) Dynamic localization cycle of the cell division regulator MinE in *Escherichia coli*. *Embo J* 20: 1563–1572.
- Lutkenhaus J (2002) Dynamic proteins in bacteria. *Curr Opin Microbiol* 5: 548–552.
- van Baarle S, Bramkamp M (2010) The MinCDJ system in *Bacillus subtilis* prevents minicell formation by promoting divisome disassembly. *PLoS One* 5: e9850.
- Gregory JA, Becker EC, Pogliano K (2008) *Bacillus subtilis* MinC destabilizes FtsZ-rings at new cell poles and contributes to the timing of cell division. *Genes Dev* 22: 3475–3488.
- Hayes F, Barilla D (2006) The bacterial segrosome: a dynamic nucleoprotein machine for DNA trafficking and segregation. *Nat Rev Microbiol* 4: 133–143.
- Fogel MA, Waldor MK (2006) A dynamic, mitotic-like mechanism for bacterial chromosome segregation. *Genes Dev* 20: 3269–3282.
- Leonard TA, Møller-Jensen J, Löwe J (2005) Towards understanding the molecular basis of bacterial DNA segregation. *Philos Trans R Soc Lond B Biol Sci* 360: 523–535.
- Funnell BE (1988) Mini-P1 plasmid partitioning: excess ParB protein destabilizes plasmids containing the centromere *parS*. *J Bacteriol* 170: 954–960.
- Ptacin JL, Lee SF, Garner EC, Toro E, Eckart M, et al. (2010) A spindle-like apparatus guides bacterial chromosome segregation. *Nat Cell Biol* 12: 791–798.
- Collier J (2012) Regulation of chromosomal replication in *Caulobacter crescentus*. *Plasmid* 67: 76–87.
- Toro E, Shapiro L (2010) Bacterial chromosome organization and segregation. *Cold Spring Harb Perspect Biol* 2: a000349.
- Thanbichler M, Shapiro L (2006) MipZ, a spatial regulator coordinating chromosome segregation with cell division in *Caulobacter*. *Cell* 126: 147–162.

23. Kieckebusch D, Michie KA, Essen LO, Löwe J, Thanbichler M (2012) Localized dimerization and nucleoid binding drive gradient formation by the bacterial cell division inhibitor MipZ. *Mol Cell* 46: 245–259.
24. Mohl DA, Gober JW (1997) Cell cycle-dependent polar localization of chromosome partitioning proteins in *Caulobacter crescentus*. *Cell* 88: 675–684.
25. Letek M, Fiuza M, Ordonez E, Villadangos AF, Ramos A, et al. (2008) Cell growth and cell division in the rod-shaped actinomycete *Corynebacterium glutamicum*. *Antonie Van Leeuwenhoek* 94: 99–109.
26. Donovan C, Schwaiger A, Krämer R, Bramkamp M (2010) Subcellular localization and characterization of the ParAB system from *Corynebacterium glutamicum*. *J Bacteriol* 192: 3441–3451.
27. Siegal-Gaskins D, Crosson S (2008) Tightly regulated and heritable division control in single bacterial cells. *Biophys J* 95: 2063–2072.
28. Aldridge BB, Fernandez-Suarez M, Heller D, Ambravaneswaran V, Irimia D, et al. (2012) Asymmetry and aging of mycobacterial cells lead to variable growth and antibiotic susceptibility. *Science* 335: 100–104.
29. Megerle JA, Fritz G, Gerland U, Jung K, Rädler JO (2008) Timing and dynamics of single cell gene expression in the arabinose utilization system. *Biophys J* 95: 2103–2115.
30. Donovan C, Sieger B, Krämer R, Bramkamp M (2012) A synthetic *Escherichia coli* system identifies a conserved origin tethering factor in Actinobacteria. *Mol Microbiol* 84: 105–116.
31. Letek M, Ordonez E, Vaquera J, Margolin W, Flärdh K, et al. (2008) DivIVA is required for polar growth in the MreB-lacking rod-shaped actinomycete *Corynebacterium glutamicum*. *J Bacteriol* 190: 3283–3292.
32. Sveiczler A, Novak B, Mitchison JM (1996) The size control of fission yeast revisited. *J Cell Sci* 109 (Pt 12): 2947–2957.
33. Bigot S, Sivanathan V, Possoz C, Barre FX, Cornet F (2007) FtsK, a literate chromosome segregation machine. *Mol Microbiol* 64: 1434–1441.
34. Lesterlin C, Barre FX, Cornet F (2004) Genetic recombination and the cell cycle: what we have learned from chromosome dimers. *Mol Microbiol* 54: 1151–1160.
35. Ramos A, Letek M, Campelo AB, Vaquera J, Mateos LM, et al. (2005) Altered morphology produced by *ftsZ* expression in *Corynebacterium glutamicum* ATCC 13869. *Microbiology* 151: 2563–2572.
36. Wachi M, Doi M, Tamaki S, Park W, Nakajima-Iijima S, et al. (1987) Mutant isolation and molecular cloning of *mre* genes, which determine cell shape, sensitivity to mecillinam, and amount of penicillin-binding proteins in *Escherichia coli*. *J Bacteriol* 169: 4935–4940.
37. Jones LJ, Carballido-Lopez R, Errington J (2001) Control of cell shape in bacteria: helical, actin-like filaments in *Bacillus subtilis*. *Cell* 104: 913–922.
38. Daniel RA, Errington J (2003) Control of cell morphogenesis in bacteria: two distinct ways to make a rod-shaped cell. *Cell* 113: 767–776.
39. Carballido-Lopez R (2006) The bacterial actin-like cytoskeleton. *Microbiol Mol Biol Rev* 70: 888–909.
40. Chastanet A, Carballido-Lopez R (2012) The actin-like MreB proteins in *Bacillus subtilis*: a new turn. *Front Biosci (Schol Ed)* 4: 1582–1606.
41. Dominguez-Escobar J, Chastanet A, Crevenna AH, Fromion V, Wedlich-Söldner R, et al. (2011) Processive movement of MreB-associated cell wall biosynthetic complexes in bacteria. *Science* 333: 225–228.
42. Garner EC, Bernard R, Wang W, Zhuang X, Rudner DZ, et al. (2011) Coupled, circumferential motions of the cell wall synthesis machinery and MreB filaments in *B. subtilis*. *Science* 333: 222–225.
43. Flärdh K (2003) Essential role of DivIVA in polar growth and morphogenesis in *Streptomyces coelicolor* A3(2). *Mol Microbiol* 49: 1523–1536.
44. Kang CM, Nyayapathy S, Lee JY, Suh JW, Husson RN (2008) Wag31, a homologue of the cell division protein DivIVA, regulates growth, morphology and polar cell wall synthesis in mycobacteria. *Microbiology* 154: 725–735.
45. Weart RB, Lee AH, Chien AC, Haeusser DP, Hill NS, et al. (2007) A metabolic sensor governing cell size in bacteria. *Cell* 130: 335–347.
46. Grover NB, Woldringh CL (2001) Dimensional regulation of cell-cycle events in *Escherichia coli* during steady-state growth. *Microbiology* 147: 171–181.
47. Ireton K, Gunther NW, Grossman AD (1994) Spo0J is required for normal chromosome segregation as well as the initiation of sporulation in *Bacillus subtilis*. *J Bacteriol* 176: 5320–5329.
48. Rodrigues CD, Harry EJ (2012) The Min system and nucleoid occlusion are not required for identifying the division site in *Bacillus subtilis* but ensure its efficient utilization. *PLoS Genet* 8: e1002561.
49. Moriya S, Rashid RA, Rodrigues CD, Harry EJ (2010) Influence of the nucleoid and the early stages of DNA replication on positioning the division site in *Bacillus subtilis*. *Mol Microbiol* 76: 634–647.
50. Harry E, Monahan L, Thompson L (2006) Bacterial cell division: the mechanism and its precision. *Int Rev Cytol* 253: 27–94.
51. Migocki MD, Freeman MK, Wake RG, Harry EJ (2002) The Min system is not required for precise placement of the midcell Z ring in *Bacillus subtilis*. *EMBO Rep* 3: 1163–1167.
52. Mohl DA, Easter J Jr, Gober JW (2001) The chromosome partitioning protein, ParB, is required for cytokinesis in *Caulobacter crescentus*. *Mol Microbiol* 42: 741–755.
53. Tauch A, Kirchner O, Löffler B, Gotker S, Pühler A, et al. (2002) Efficient electrotransformation of *Corynebacterium diphtheriae* with a mini-replicon derived from the *Corynebacterium glutamicum* plasmid pGA1. *Curr Microbiol* 45: 362–367.
54. Schäfer A, Tauch A, Jäger W, Kalinowski J, Thierbach G, et al. (1994) Small mobilizable multi-purpose cloning vectors derived from the *Escherichia coli* plasmids pK18 and pK19: selection of defined deletions in the chromosome of *Corynebacterium glutamicum*. *Gene* 145: 69–73.